MAGNETIC RESONANCE IN CHEMISTRY
*Magn. Reson. Chem.* **36**, 839–847 (1998)

# Long-range proton–carbon coupling constants in conformational analysis of oligosaccharides

**Torgny Rundlöf,[1] Alexandra Kjellberg,[1] Charlotta Damberg,[2]† Toshiaki Nishida[2] and Göran Widmalm[1]***

[1] Department of Organic Chemistry, Arrhenius Laboratory, Stockholm University, S-106 91 Stockholm, Sweden
[2] Swedish NMR Centre, Stockholm, Sweden

*Received 19 February 1998; Revised 10 May 1998; Accepted 18 May 1998*

ABSTRACT: Long-range heteronuclear coupling constants, $^3J$(C,H), were measured across glycosidic linkages in $\beta$-linked disaccharides and also for vicinally disubstituted trisaccharides. One-dimensional multiple-site $^{13}$C excitation experiments using Hadamard spectroscopy and band-selective $^1$H decoupling during the acquisition period were used in conjunction with pulsed field gradients for coherence selection in the $^1$H detected experiment. For one dihedral angle the $^3J$(C,H) value could only be unambiguously determined utilizing the band-selective $^1$H decoupling. The 2D EXSIDE was also used for the measurement of $^3J$(C,H) values and the results showed excellent agreement with those of the 1D measurements. The influence of solvent, water and water–dimethyl sulfoxide (7:3), on conformation was investigated, but showed only small changes in $^3J$(C,H) values. In general, the long-range heteronuclear coupling constants related to the $\phi$ dihedral angles (3.6–4.3 Hz) were smaller than those of the $\psi$ dihedral angles (4.3–5.3 Hz). A comparison with $^3J$(C,H) values from Monte Carlo or Langevin dynamics simulations showed better agreement for the $\psi$ dihedral angles than for the $\phi$ dihedral angles as calculated using a Karplus relationship. © 1998 John Wiley & Sons Ltd.

KEYWORDS: NMR; $^1$H NMR; $^{13}$C NMR; long-range $^{13}$C–$^1$H coupling constants; time-shared homonuclear decoupling; oligosaccharides; Hadamard spectroscopy; *J*-doubling; Langevin dynamics

## INTRODUCTION

A large number of structural combinations are possible when monosaccharide residues are linked into oligo- or polysaccharides. As a result, carbohydrates are used as signal substances in biological systems. Along with the geometries of the constituent monosaccharide residues, the linkages between the sugar residues are of great importance in determining the three-dimensional structure of saccharides and the biologically active conformation. In the conformational analysis of oligosaccharides in solution, NMR spectroscopy is valuable for obtaining information about the three-dimensional structure. The studies are usually based on measurements of nuclear Overhauser effects (NOE) and long-range heteronuclear coupling constants. This is the case for both the intra-residue conformation, i.e. of each monosaccharide, and in particular for the inter-residue conformation(s) between the constituent monosaccharides. The measurable NOEs across a glycosidic linkage are usually limited to just a few, the most pronounced commonly being that between the anomeric proton on one residue and the proton on the substitution carbon of the next sugar residue. By the use of sugar hydroxyl protons in aprotic solvents, such as dimethyl sulfoxide (DMSO), more trans-glycosidic NOEs can be observed.[1] Additional data are usually needed for an extensive conformational analysis of an oligosaccharide. Long-range heteronuclear coupling constants across the glycosidic linkage can supply complimentary information when interpreted by a Karplus-type relationship,[2] i.e. $J = A\cos^2\theta + B\cos\theta + C$, where $\theta$ defines the torsional angle and $A$, $B$ and $C$ are constants. Although a $^3J$(C,H) value cannot be interpreted from a Karplus curve as a single averaged dihedral angle without additional information on the conformational space accessible to the molecule, it still offers valuable information in conjunction with other techniques such as molecular modeling. Two recent parameterizations of Karplus type relationships for the glycosidic linkage of saccharides[3,4] showed only minor differences and either of them can then be used to relate measured $^3J$(C,H) values to averaged torsional angles.

Early measurements of long-range heteronuclear coupling constants include those within the sugar ring and those of methyl glycosides.[5] Later, the measurements were extended to oligosaccharides for which the coupling constants related to the glycosidic torsional angles $\phi$ and $\psi$ were obtained.[6] Measurements were also performed on specifically $^{13}$C [7] or $^2$H-labelled[8] substances. Subsequent development in NMR techniques for the measurement of long-range heteronuclear coupling constants include 2D proton-flip[9] and 2D DEPT experiments.[10] More recently, methods have applied 2D proton-detected experiments.[11–13] One-

* *Correspondence to*: G. Widmalm, Department of Organic Chemistry, Arrhenius Laboratory, Stockholm University, S-106 91 Stockholm, Sweden.
† *Present address*: Swedish NMR Centre at Göteborg University, Hasselblad Laboratory, S-413 90 Gothenburg, Sweden.
*Contract/grant sponsor*: Swedish Natural Science Research Council.

 CCC 0749-1581/98/110839–09 $17.50

dimensional experiments[14–18] for selective $^{13}C$ excitations have been performed by using shaped pulses.[19] The selective excitation may also be performed simultaneously for multiple sites by the application of Hadamard spectroscopy,[20,21] where the relative sign of each selective pulse is set according to a Hadamard matrix. Time-shared homonuclear decoupling in band-selective or single-frequency mode during the acquisition period[22] leads to a 50% increase in the signal-to-noise ratio and a more straightforward interpretation of spectra. The use of gradient selection in pulse sequences for the measurement of long-range heteronuclear coupling constants is currently being pursued by several groups[23–26] since artefact-free spectra result from the application of pulsed field gradients (PFGs). Some of these techniques mentioned above are applicable only to protonated carbons. In the present investigation, we chose methods which are applicable to all types of carbons, including non-protonated carbons.

The numerical value of the long-range heteronuclear coupling constant can be extracted by different methods depending on the complexity of the spectra from the investigated compound and the experimental techniques used. The coupling constant can readily be obtained by direct measurement of the in-phase[26] or anti-phase[14] peak-to-peak separation due to splitting of the NMR signal if spectral overlap is not severe, multiplicity is low and the linewidths are small in comparison with the measured splitting. When multiplicity is complex or the linewidth exceeds the coupling constant, one will have to rely on techniques such as the evaluation of an integral[27] as in the *J*-doubling procedure[14,28] or the scaling factor approach.[12,26,29]

Long-range carbon–proton coupling constants have frequently been used in structural studies and conformational analysis[30,31] and their application to saccharides has recently been reviewed by Tvaroska and Taravel.[32] In the present work we investigated long-range carbon–proton coupling constants across the glycosidic linkage of vicinally disubstituted trisaccharides, disaccharide analogues thereof and a site-specifically deuterated disaccharide. One of the trisaccharides has recently been found as the repeating unit of the exopolysaccharide from a strain of *Pedicoccus damnosus*.[33] The measurements were performed in aqueous solutions and also in a cryo-solvent consisting of water–DMSO (7:3)[34] since, in previous work, we used the cryo-solvent for multiple field $^{13}C$ relaxation studies.[35–40] The measured $^{3}J(C,H)$ values were interpreted using a Karplus-type relationship and subsequently compared with those calculated for the oligosaccharides using Langevin dynamics[41,42] and Monte Carlo simulations.[43]

## EXPERIMENTAL

### General

The oligosaccharides studied were methyl β-D-Glc*p*-(1 → 2)-[β-D-Glc*p*-(1 → 3)]-α-D-Glc*p* (**1**), methyl β-D-Glc*p*-(1 → 2)-[β-D-Glc*p*-(1 → 3)]-α-D-Man*p* (**2**), methyl β-D-Glc*p*-(1 → 2)-α-D-Glc*p* (**3**), methyl β-D-Glc*p*-(1 → 3)-α-D-Glc*p* (**4**), methyl β-D-Glc*p*-(1 → 2)-α-D-Man*p* (**5**), methyl β-D-Glc*p*-(1 → 3)-α-D-Man*p* (**6**) and methyl-$^{2}H_3$ β-D-Glc*p*-3,5,6,6′-$^{2}H_4$-(1 → 4)-β-D-Glc*p*-3,5,6,6′-$^{2}H_4$ (**7**). Five of these were used for NMR measurements; their syntheses have been reported previously, i.e. **1**, **2**, **6**,[44] **5**[45] and **7**.[46]

### NMR spectroscopy

The oligosaccharides were dissolved in $D_2O$ or in $D_2O$–DMSO-$d_6$ (molar ratio 7:3), to concentrations of 50–120 mM. NMR spectra were recorded at 30 °C on a Varian Unity 500, a Varian Unity Plus 600 or a Varian Inova 600 NMR spectrometer equipped with a 5 mm triple resonance PFG probe. Measurements of long-range $^{13}C$–$^{1}H$ coupling constants were performed using the multiple $^{13}C$ site-selective excitation experiment according to the procedure of Blechta *et al.*,[14] with extensions which included time-shared band-selective proton decoupling with a duty cycle of 0.2 during the acquisition and PFGs for coherence selection and suppression of artefacts as devised by Nishida *et al.*[22,23] Typically, the time of the delay between excitation and coherence transfer, to allow for evolution of the long-range coupling, was set to 30 ms. Hadamard shapes,[20] for two and four sites, were generated by using the program Pandora's Pulse Box.[47] Half-Gaussian shaped pulses[48] of 25 or 50 ms duration were used for selective $^{13}C$ excitation and band-selective homonuclear decoupling was achieved with i-BURP-2[19] or i-SNOB-3[49] shaped pulses. The two gradients were applied prior to and after the last pair of 90° pulses. The amplitudes of the gradients were typically set to 21 G $cm^{-1}$, with durations of 2 and 0.5 ms, respectively. Spectral widths of 2000–5000 Hz were sampled with 16 384–32 768 data points using 500–8000 transients for each Hadamard excitation. FIDs were processed using VNMR software (Varian Associates). Zero-filling eight times and multiplication of the FID with an exponential weighting function with a line broadening factor of 0.3–0.6 Hz was applied prior to Fourier transformation. The *J*-doubling procedure[50] used eight or 16 delta functions in the frequency domain. The error of the determined value of the coupling constants was estimated to be not greater than 0.2 Hz based on a digital resolution of 0.12–0.20 Hz in the spectra.

The 2D EXSIDE[26] spectrum was recorded using a Gaussian cascade Q3 pulse[51] of 14 ms duration for selective inversion of the two β-glucosidic anomeric protons in **2** and spectral widths of 3000 and 1000 Hz for $^{1}H$ and $^{13}C$, respectively. A *J*-scaling factor of 10 was used and 16 scans of 2048 complex data points were collected for 512$t_1$ increments. Prior to Fourier transformation the spectrum was zero-filled to 2048 × 4096 data points and multiplied by a Gaussian function in both dimensions.

 

## Computational procedures

Simulations were performed on **1**–**6** using three different force fields, namely HSEA,[52] CHEAT95[53] and PARM22 (MSI, San Diego, CA, USA). The first employed Metropolis Monte Carlo (MMC) simulations[43] and the other two CHARMm[54]-based types used Langevin dynamics (LD) simulations,[41,42] which is a molecular dynamics based method in which the solvent is modeled by random and frictional forces. The dihedral angles $\phi$ and $\psi$ were defined as: $\phi$ = H-1′—C-1′—O-1′—C-X and $\psi$ = C-1′—O-1′—C-X—H-X, where X is the linkage position, which is also indicated by a subscript. All simulations were performed at 300 K. Heteronuclear coupling constants were calculated using the Karplus relationship as devised by Tvaroska *et al.*[4] ($A = 5.7$, $B = -0.6$, $C = 0.5$) for each saved conformation and subsequently averaged.

As reported earlier,[44] MMC simulations were performed using the GEGOP program,[55] version 2.6, and the HSEA force field. The maximum step length for the dihedral angles $\phi$ and $\psi$ was set to 20°. A total of $10^6$ macro steps were performed for each of the molecules with an acceptance ratio between 30 and 60%.

LD simulations were performed using the CHARMm program (MSI), version 4.0, and the CHEAT95 or PARM22 force fields. LD includes a collision frequency $\gamma = \zeta/m$, where $\zeta$ is the friction constant and $m$ is the atomic mass. A value of $\gamma = 50$ ps$^{-1}$ was applied to carbons and oxygens, as described previously.[42]

A 5 ns simulation was performed for each of the molecules. For PARM22 a dielectric constant ($\varepsilon$) of unity was used, which for a similar CHARMm-based force field gave a better agreement with $^1$H,$^1$H NOE experimental data than did a high value ($\varepsilon = 80$).[42] A distance-dependent dielectric was used for CHEAT95 as described.[53] A time step of 1.0 fs was employed and data sampling took place every 0.1 ps for analysis.

The major difference between the CHEAT95 and PARM22 force fields is that the former uses extended atoms for the representation of hydroxyl groups which simulates the averaged effect of intra- and intermolecular hydrogen bonding.

## RESULTS AND DISCUSSION

Long-range heteronuclear coupling constants, $^3J$(C,H), across glycosidic linkages were measured for trisaccharides **1** and **2** and disaccharides **5**–**7**. The experimental data were compared with those obtained from Monte Carlo and molecular dynamics simulations, in order to investigate the three-dimensional structure and the conformational flexibility of the oligosaccharides. The influence of a solvent change on the measured parameter was also addressed.

For the measurement of $^3J$(C,H) values we used 1D $^{13}$C multi-site excitation experiments,[14,22,23] employing a Hadamard scheme. PFGs were used to facilitate measurement of resonances at or close to solvent signals as well as to suppress artefacts. Time-shared band-selective decoupling of proton(s) adjacent to the proton used for detection was employed during the acquisition period in order to reduce the multiplicity and thereby simplify the extraction of the heteronuclear coupling constant. Long-range proton–carbon coupling constants were extracted using the *J*-doubling method.[14,28] The 2D EXSIDE (see below) was applied to trisaccharide **2** and values of the long-range heteronuclear coupling constants were measured directly in the spectrum. The values of all measured coupling constants are given in Table 1.

In Fig. 1 the atoms of interest for the measurement of $^3J$(C,H) values across the glycosidic linkages are shown. These include anomeric and glycosylation carbons for selective excitations and anomeric protons and protons at glycosyloxylated carbons, i.e. linkage carbons. Furthermore, protons that were irradiated in order to obtain decoupling of observed signals are also depicted. Trisaccharides **1** and **2** contain four sites for excitation and disaccharides **5** and **6**, which are the constituent

**Table 1.** Experimental heteronuclear long-range coupling constants (Hz) of oligosaccharides **1**, **2** and **5**–**7** in different solvents

| | | $D_2O$ | | $D_2O$:DMSO | |
|---|---|---|---|---|---|
| Substance | Linkage | $^3J$(H-1,C-X)[a] | $^3J$(C-1,H-X) | $^3J$(H-1,C-X) | $^3J$(C-1,H-X) |
| **1** | 2 | 3.8; 3.8[b] | 4.5; 4.5[c] | 3.7 | 4.9 |
| | 3 | 3.9 | 4.9 | 4.0 | 4.9 |
| **2** | 2 | 4.1; 4.1[b]; 4.1[d] | 5.1[e] | 4.3[b] | 5.0[e] |
| | 3 | 3.7; 3.6[b]; 3.7[d] | 4.3 | 3.6[b] | 4.3 |
| **5** | 2 | 4.1; 4.1[b] | 5.3[e] | — | — |
| **6** | 3 | 4.1[b] | 4.5 | — | — |
| **7** | 4 | 4.1 | 5.3 | 4.2 | 5.2 |

[a] X = linkage position.
[b] Band-selective decoupling of H-2 in glucosyl groups.
[c] Band-selective decoupling of H-1 in the α-glucosyl residue.
[d] Coupling constant obtained using EXSIDE.
[e] Band-selective decoupling of H-1 in the α-mannosyl residue.

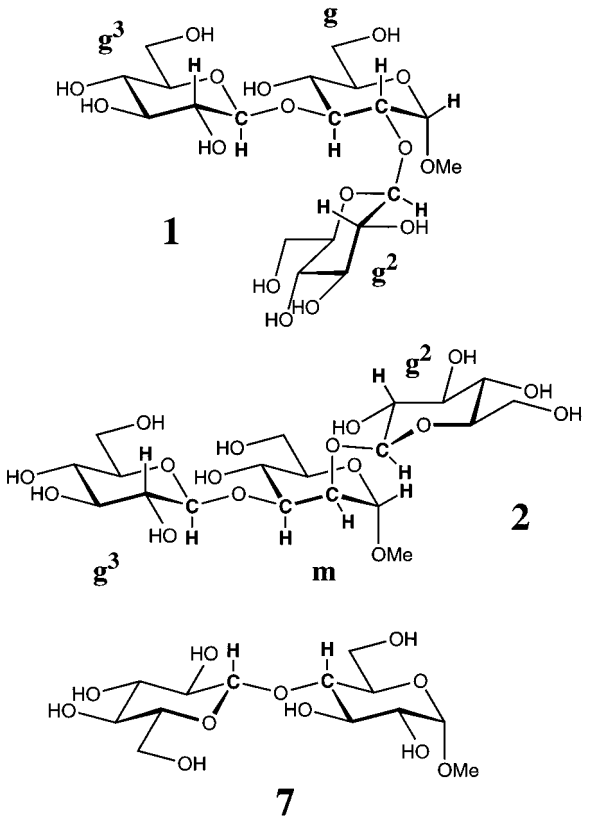


**Figure 1.** Three of the oligosaccharides studied. Carbons selectively excited are indicated in the molecules, as are protons that were used to detect the long-range coupling constant across the glycosidic linkage or that were band-selectively decoupled during the acquisition period. Trisaccharides **1** and **2** consist of two terminal $\beta$-glucosyl residues substituted at positions 2 (residue $\mathbf{g}^2$) and 3 (residue $\mathbf{g}^3$) of a methyl glucoside (**g** in structure **1**) or a methyl mannoside (**m** in structure **2**).

disaccharides of trisaccharide **2**, and also disaccharide **7**, contain two excitation sites.

The multiple-site selective excitations, two and four sites in this study, were performed using half-Gaussian-shaped pulses with different phase (0° or 180°) at the different excitation frequencies. In this way each experiment results in two or four traces. Appropriate combinations of additions and subtractions of the different traces according to the Hadamard matrix (+ + and + − for two sites) produce spectra from which couplings from a single site can be identified and measured. This Hadamard encoding and decoding results in an increase of signal to noise of $n^{1/2}$, where $n$ is the number of sites, compared with single-site excitation in a given experimental time.[14]

In $D_2O$ the C-2 and C-3 signals of the **g** residue in trisaccharide **1** were separated by only 18 Hz in the 150 MHz $^{13}C$ spectrum and a shaped pulse with a duration of 25 ms was used to excite both carbons at the same time. The chemical shifts of the anomeric proton resonances used for detection differed sufficiently to obtain non-overlapping multiplets with long-range anti-phase splittings.

The 1D pulse sequence used is of the inverse type,[14,22,23] in which the delay time between the selective $^{13}C$ excitations and the coherence transfer to the protons for detection is set for the measurement of $^3J$(C, H) couplings. The delay time is usually set for optimum transfer of a larger coupling constant (in this case *ca.* 17 Hz) than the actual value of the long-range coupling constant (in this case *ca.* 4–5 Hz). The detected signals show opposite phase for the homonuclear and the heteronuclear couplings, i.e. the $^1H,^1H$ couplings are observed in phase and the $^1H,^{13}C$ couplings are thus in anti-phase (Fig. 2). In general, when the heteronuclear coupling constant to be measured is $>1.5$ times the observed linewidth, the extraction of the $^nJ$(C,H) values can be performed in a straightforward manner,[56] provided that the homonuclear coupling constant is not of the same size as the heteronuclear coupling constant, which will lead to cancellations in the spectrum. The proton multiplicity, which is present in most cases, will make the extraction of the $^nJ$(C,H) values more complicated. Five different multiplicities were present at the detected protons of trisaccharides **1** and **2**. The anomeric proton of the $\beta$-glucosyl residues was split to a doublet by a *ca.* 8 Hz homonuclear coupling to H-2

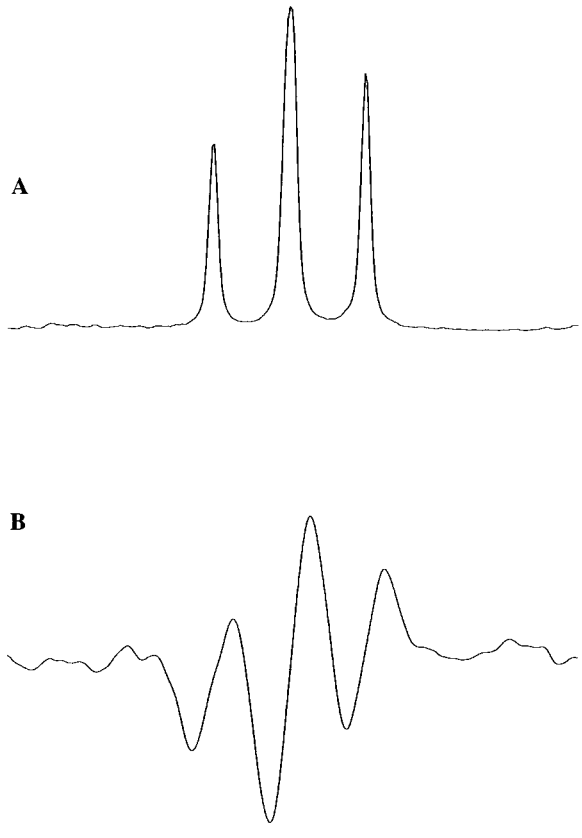


**Figure 2.** (A) Part of the $^1H$ NMR spectrum of **1**, showing the signal from H-3 in the **g** residue. This signal is split due to $J$(H-3,H-2) and $J$(H-3,H-4). (B) The $^1H$ NMR spectrum resulting from the long-range experiment with selective excitation of C-1 in the $\mathbf{g}^3$ residue. The H-3 signal is further split into anti-phase by the long-range heteronuclear coupling between C-1 in $\mathbf{g}^3$ and H-3 in **g**, related to the $\psi$ dihedral angle.

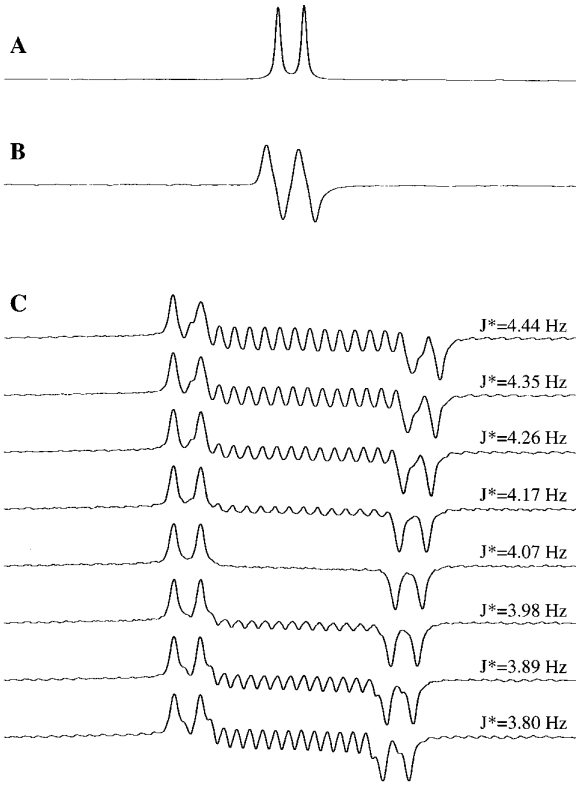


**Figure 3.** (A) Part of the $^1$H NMR spectrum of **2**, expanded to show the anomeric proton [$J$(H-1,H-2) = 8 Hz] of the $\mathbf{g}^2$ residue. (B) The $^1$H NMR spectrum showing H-1 in $\mathbf{g}^2$ obtained after the long-range experiment with selective excitation of C-2 in the **m** residue. The in-phase split signal is further split by a 4.1 Hz anti-phase contribution due to the long-range coupling, related to the $\phi$ dihedral angle. (C) The $J$-doubling procedure has been performed, and the in-phase doublet is separated by eight times $J$*, the trial coupling constant. When $J^* = J$ (4.07 Hz), the integral has reached its minimum value and the characteristics of the in-phase proton doublet are retained.

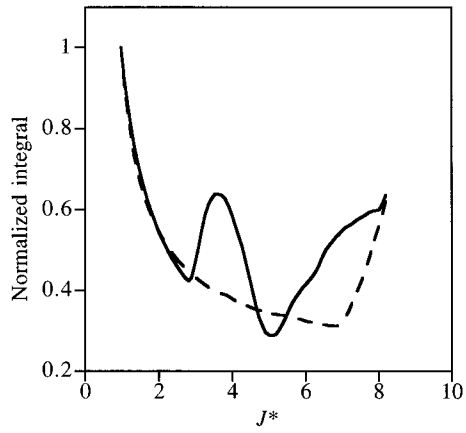


**Figure 4.** Output from $J$-doubling ($J$* *vs.* normalized integral) of the signal resulting from the long-range experiment with excitation of C-1 in the $\mathbf{g}^2$ residue and detection of H-2 in the **m** residue of **2** in $D_2O$. It was impossible to extract the value of the long-range coupling constant for this dihedral angle from the observed multiplet (dashed line), but with time-shared decoupling of H-1 of residue **m** during acquisition (solid line) the value of the coupling constant was readily determined.

[Fig. 3(A) and (B)]. In the methyl glycosides, H-2 and H-3 were split to doublets of doublets with $^3J$(H,H) values of 2–9 Hz (Fig. 2).

For all extracted $J$-values, the $J$-doubling procedure was used, in which an integral global minimum is sought which also retains the correct proton multiplicity [Fig. 3(C)]. The extracted values were in good agreement with those measured directly from the anti-phase separation in well resolved proton-detected signals. Band-selective decoupling during the acquisition period was also applied to some protons, which led to a reduced multiplicity of the signal and a 50% increase in the signal-to-noise ratio. The agreement between the measurement with and without band-selective decoupling during acquisition is excellent and within the experimental error ($\pm$0.2 Hz). In one case, i.e. between C-1 of $\mathbf{g}^2$ and H-2 of **m** in **2** in water and in the cryosolvent, and also in **5**, the value of $^3J$(C,H) could only be obtained after decoupling of the anomeric proton of the mannosyl residue (Fig. 4). For this linkage both $J$(H-1,H-2) and $J$(H-2,H-3) were small (1.8 Hz and 3.1 Hz, respectively). The former is about one third the size of $^3J$(C,H), and the latter is approximately two thirds of the long-range coupling constant. This combination resulted in several, from each other indistinguishable, local integral minima and an apparent global minimum of 7 Hz. When H-1 of the **m** residue was selectively decoupled during the acquisition, one local and one global minima were found by the $J$-doubling procedure. The global minimum was found to show the correct proton multiplicity.

The method used above involves measurements of the long-range coupling constants in the presence of homonuclear couplings. EXSIDE[26] (*ex*citation-sculptured *i*ndirect-*d*etection *e*xperiment), which is a band-selective version of the gradient-enhanced HSQC experiment, produces a pure-absorptive spectrum in both the $F_1$ and $F_2$ dimension. The cross peak appears as a doublet in the $F_1$ dimension, with a peak-to-peak separation of the long-range CH coupling constant scaled up by the pre-defined $J$ scaling factor. In the $F_2$ dimension the signals are only split due to passive homonuclear proton couplings, since the $^{13}$C nuclei are decoupled during the acquisition period. The possibility to measure the long-range couplings without the interference of passive couplings is due to the fact that only proton resonances that do not have any homonuclear coupling between them are band-selectively excited.

EXSIDE was applied to **2**. The anomeric protons of the glucosyl residues were band-selectively excited to measure the heteronuclear coupling constants for the $\phi$ dihedral angles. An expansion from the EXSIDE spectrum is shown in Fig. 5. The frequency separation using a $J$-scaling factor $N = 10$ gives $^3J$(C,H) values, listed in Table 1, which showed excellent agreement with the values obtained from the 1D experiment.

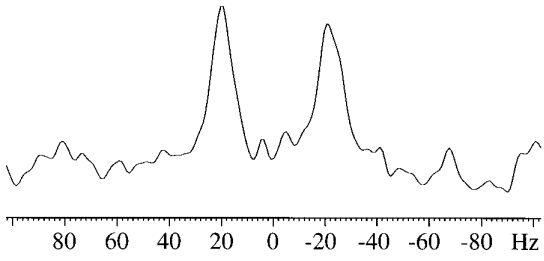


**Figure 5.** Trace from the 2D EXSIDE spectrum of **2**, using a scaling factor of 10. The trace was taken at the $F_2$ chemical shift of H-1 in the **g**$^2$ residue and then expanded in the $F_1$ dimension to show the signal of C-2 in the **m** residue. The signal is split into a doublet of 41 Hz, i.e. 10 times $J$ related to the $\phi$ value.

In spite of the experimental time penalty for a 2D method, direct measurement of the long-range coupling constant in the absence of homonuclear couplings could be performed in cases where the 1D method used above produce ambiguous results. The prerequisite that excited protons cannot have a common homonuclear coupling limits the applicability and no long-range heteronuclear coupling constants for the $\psi$ dihedral angles were measured using this method. However, the EXSIDE and the 1D multiple site selective excitation experiments complement each other, especially for carbohydrates, where the signals from the anomeric atoms usually are resolved whereas the signals from ring atoms often overlap. Thus, the 1D sequence is preferably used to measure the long-range coupling constant for the $\psi$ dihedral angle (selectively exciting the often well resolved anomeric carbon signal) and, in cases where there is overlap at the chemical shift of the glycosylation carbons, EXSIDE is used for measurement of the long-range coupling constant for the $\phi$ dihedral angle (band-selectively exciting the often well resolved anomeric proton signals).

In studies of carbohydrate dynamics, we used $^{13}$C NMR relaxation data to probe the overall and internal correlation times and the degree of internal motions.[35–40] In these studies a cryo-solvent of water–DMSO (molar ratio 7:3) was used.[34] For trisaccharides **1** and **2** and disaccharide **7**, the $J$-values were measured across the glycosidic linkages in solutions of this cryo-solvent and also in solutions of $D_2O$. The measured $J$-values in the solvent mixture are almost invariant from those obtained in water solution. They are within the experimental error of the technique, although the value for the $\psi$ torsional angle of the (1 → 2)-linkage in **1** is at the limit of the experimental error. Provided that the conformational flexibility is similar in the two solvents, this can be interpreted as if only small changes of conformations have taken place by change of solvent. Thus, the overall conformation and three-dimensional shape of the oligosaccharides should not have been perturbed to any great extent by the change to the cryo-solvent, which still contains 70% of water. In addition, trans-glycosidic $^3J$(C,H) values for α-L-Rha*p*-(1 → 2)-α-L-Rha*p*-OMe do not show large differences between water and DMSO as solvent.[57] The interpretation is also in agreement with relative $^1$H,$^1$H NOEs, which do not show large changes in oligosaccharides dissolved in water as compared with DMSO or pyridine[58] or to the cryo-solvent.[59] Therefore, to a good approximation the cryo-solvent is an alternative to water when low-temperature experiments need to be performed.

In all compounds the trans-glycosidic $^3J$(C,H) are smaller for the $\phi$ dihedral angles, 3.6–4.3 Hz, than for the $\psi$ dihedral angles, 4.3–5.3 Hz. The range of values are also smaller for the former. In **1** the $^3J$(C,H) values related to the $\phi$ dihedral angle are similar for the 2- and 3-linkages, whereas in **2** a difference of *ca.* 0.5 Hz is observed for these linkages. Similar changes take place for the $^3J$(C,H) values related to the $\psi$ dihedral angles, i.e. in **1** the differences are smaller whereas in **2** they are larger. In previous studies of **1** and **2** employing MMC simulations[44] and $^{13}$C NMR relaxation measurements,[40] the two glycosidic linkages in **1** showed similar conformational and motional properties whereas in **2** they differed. A comparison between trisaccharide **2** and its constituent disaccharide **5** revealed that the (1 → 2)-linkage shows similar $^3J$(C,H) values. For the (1 → 3)-linkage, trisaccharide **2** and disaccharide **6** show a difference of *ca.* 0.5 Hz in the observed $^3J$(C,H) values associated with the $\phi$ dihedral angle, whereas the value related to the $\psi$ dihedral angle is similar in the two compounds.

For a given $J$-value the averaged oligosaccharide conformation can be interpreted via the Karplus relationship, in most cases as four possible values of the dihedral angle since the Karplus equation is $\cos^2\theta$ modulated. These four possible conformations, along with the fact that only the time-averaged conformation may be extracted from the $J$-values, make the interpretation of long-range carbon–proton coupling constants in terms of detailed information about the conformation at the glycosidic linkages difficult. To correlate the measured $J$-values to time-averaged 3D structures we performed Monte Carlo (MC) and molecular dynamics simulations. The averaged $J$-values from the different computer simulations, calculated from each saved conformation, were compared with the measured $J$-values.

The molecular modeling employed the HSEA force field for the MC simulations. Two force fields, PARM22 and CHEAT95, were used in the Langevin dynamics (LD) simulations. In the present case good averaging of the parameter of interest, $^3J$(C,H), is estimated to have taken place in the region around the global energy minimum for the MC simulations and a sufficient number of transitions in the LD simulations in order to make a comparison valid for the experimental values. It is conspicuous that the $^3J$(C,H) values related to the $\phi$ dihedral angle are substantially and systematically underestimated, irrespective of the force field used (Table 2, Fig. 6). For the $\psi$ dihedral angles the fit is much better and in some cases excellent. The simulations showed significant differences in the calculated $^3J$(C,H) values between trisaccharide **2** and its constituent disaccharides **5** and **6** for $\phi_2$ and $\phi_3$ using the PARM22 force field and for $\psi_2$ with the CHEAT95

 

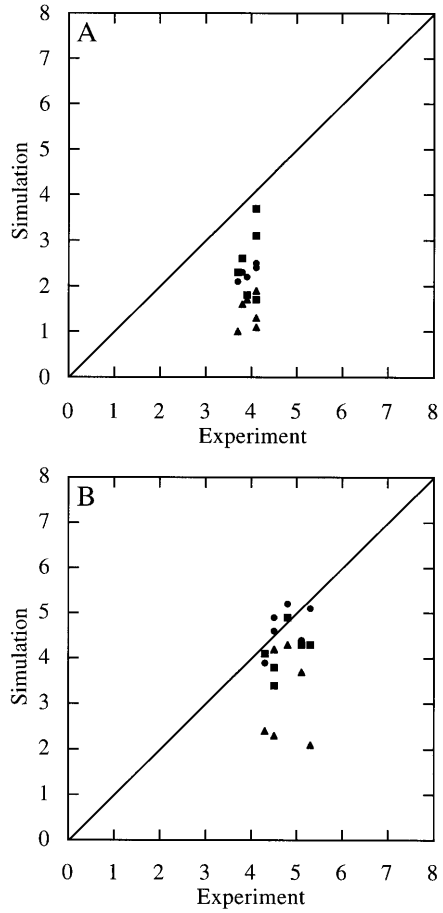


**Figure 6.** Comparison between coupling constants measured in the experiment and coupling constants calculated from the simulations with different force fields, namely HSEA (●), PARM22 (■) and CHEAT95 (▲). In (A) the values for the coupling constants related to $\phi$ do not show very good agreement between experiment and simulation, whereas in (B) the agreement between experiment and simulation related to $\psi$ is much better.

force field. These large changes are not observed in the experimental values of $^3J$(C,H) for trisaccharide **2** and disaccharides **5** and **6**. A number of large differences in the calculated $^3J$(C,H) values occur between the three force fields. This is particularly notable for the CHARMm-based force fields, e.g. $\psi_3$ in **2** and $\psi$ in **5** show large differences between CHEAT95 and PARM22. From the simulations it was observed that the $\phi$ dihedral angles populate the region of the first quadrant (0–90°), as major or exclusive conformations. The PARM22 force field showed an '*anti*'-conformer ($\phi \approx 180$)[60,61] to be present occasionally at the $\beta$-(1 → 2)-linkages. For $\psi$ both positive (first quadrant) and negative angles (fourth quadrant) were observed. The interpretation of $^3J$(C,H) values across the glycosidic linkage has been based on the same Karplus-type relationship for both $\phi$ and $\psi$ even though the substituents at the carbon atoms are different with respect to the $\phi$ and $\psi$ dihedral angles. This may be a reason for the discrepancy in $\phi$, which using three different force fields is systematically underestimated, although the conformational behavior of a given molecule is similar between force fields. A modification of the present Karplus relationships into one for $\phi$ and one for $\psi$ is therefore warranted and highly desirable.

Although differences in the comparison of $^3J$(C,H) values between experiment and simulation can be identified in this study, further investigattions are needed to differentiate properly the carbohydrate force fields. Other experimental data should also be used, such as $^1$H,$^1$H NOEs at different magnetic field strengths and in different solvents. In addition, similar studies of oligosaccharide conformation with comparison to trans-glycosidic $^3J$(C,H) values are being extended to other systems. Previously, the $^3J$(C,H) values measured for methyl α-D-Man*p*-(1 → 2)-β-D-Glc*p* could be reproduced in an excellent way,[62] i.e. to within the experimental error of the technique, using two force fields (HSEA and PARM22) with marked differences in conformational flexibility.

The trans-glycosidic heteronuclear coupling constants in methyl β-cellobioside have also been measured. A site-specifically deuterated analogue, methyl-$^2H_3$β-D-Glc*p*-3,5,6,6′-$^2H_4$-(1 → 4)-β-D-Glc*p*-3,5,6,6′-$^2H_4$ (**7**), was used. This facilitated accurate measurements, in particular for $^3J$(C,H) related to $\psi$, since H-3, H-4 and H-5 of the undeuterated compound have similar chemical

**Table 2.** Calculated heteronuclear long-range coupling constants (Hz) of oligosaccharides **1–6** from MMC and LD simulations

| | | Force field | | | | | |
|---|---|---|---|---|---|---|---|
| | | HSEA | | PARM22 | | CHEAT95 | |
| Substance | Linkage | $^3J$(H-1,C-X)[a] | $^3J$(C-1,H-X) | $^3J$(H-1,C-X) | $^3J$(C-1,H-X) | $^3J$(H-1,C-X) | $^3J$(C-1,H-X) |
| **1** | 2 | 2.3 | 4.9 | 2.6 | 3.4 | 1.6 | 4.2 |
| | 3 | 2.2 | 5.2 | 1.8 | 4.9 | 1.7 | 4.3 |
| **2** | 2 | 2.5 | 4.4 | 3.1 | 4.3 | 1.9 | 3.7 |
| | 3 | 2.1 | 3.9 | 2.3 | 4.1 | 1.0 | 2.4 |
| **3** | 2 | 2.6 | 4.8 | 2.5 | 2.8 | 1.9 | 3.9 |
| **4** | 3 | 2.4 | 5.3 | 2.1 | 4.3 | 1.5 | 4.6 |
| **5** | 2 | 2.4 | 5.1 | 1.7 | 4.3 | 1.1 | 2.1 |
| **6** | 3 | 2.4 | 4.6 | 3.7 | 3.8 | 1.3 | 2.3 |

[a] X = linkage position.

shifts ($\delta_H$ 3.60–3.63)[63] and the proton–proton coupling constants from H-4 are large (*ca.* 10 Hz). In the deuterated analogue, where C-3 and C-5 carry $^2$H, the coupling constants from H-4 to the deuterons should be small. In practice, the H-4 proton of **7** in $D_2O$ only show a single resonance with $v_{1/2} \approx 2$ Hz, twice the natural linewidth in the $^1$H NMR spectrum at 600 MHz.

Gradient selection facilitated a clean measurement on the anomeric proton, since residual HDO was present close to the resonance of the anomeric proton. In the same manner as for the above $\beta$-linked glucosyl residues of **1** and **2**, the signal from the anomeric proton of the glucose group showed an in-phase splitting of *ca.* 8 Hz deriving from $J$ coupling to its H-2. From the anti-phase splitting in the multiplet a long-range coupling constant of 4.1 and 4.2 Hz in water and water–DMSO, respectively, could be derived using the $J$-doubling procedure. The magnitude of this $^3J$(C,H) can subsequently be related to the $\phi$ dihedral angle. The $^3J$(C,H) value related to the $\psi$ dihedral angle could be obtained from the anti-phase splitting of the H-4 resonance, showing values of 5.3 and 5.2 Hz in water and in the cryosolvent, respectively.

The $^3J$(C,H) value related to $\phi$ shows in the present study excellent agreement with previous studies.[6,8] However, for the $^3J$(C,H) value related to $\psi$ and measured from the site-specifically deuterated analogue, in which the elimination of $^1$H,$^1$H couplings leads to a straightforward identification of the anti-phase splitting, a larger $^3J$(C,H) value could be extracted, the difference being up to *ca.* 1 Hz compared with earlier studies.[6,8] The range of the Karplus curve for these C—O—C—H dihedral angles is *ca.* 1–7 Hz, and the above difference in $^3J$(C,H) may have consequences for the interpretation of the $^3J$(C,H) values in the conformational studies of carbohydrates, as will be discussed below.

Cellobiose was recently studied by energy minimization and molecular dynamics simulations.[64] Conformational averages over different $\phi/\psi$ regions and a number of dynamics-averaged models were evaluated by comparison with optical rotation and heteronuclear trans-glycosidic coupling constants. The dynamics-averaged models also investigated the effects of differences in the treatment of oxygen lone pairs, dielectric constants and force fields. For the cellobiose simulation study the comparison of $^3J$(C,H) values was made based on NMR data from Hamer *et al.*[8] A single conformation did not fit the data, but a fairly equal conformational distribution between the two low-energy minima did. Additional higher energy minima were judged to contribute to only a minor extent. The simulation of cellobiose in water showed only a slight influence of the solvent on the conformation and flexibility in different energy wells.[65] However, if interpretation of the simulation data is made for $\psi$ having a larger $^3J$(C,H) value, as in the present measurement, the contribution of other energy minima such as an '*anti*'-conformer ($\psi \approx 180°$) will be increased,[66,67] as will subsequently the flexibility of the glycosidic linkage in the disaccharide.

In conclusion, measured values of $^3J$(C,H) are readily obtained using gradient selection and multiple site $^{13}$C selective excitation 1D experiments[14] with the improvements devised by Nishida *et al.*,[22,23] followed by the $J$-doubling procedure[14,28] for extraction of spin–spin coupling constants. PFGs for coherence selection resulted in clean and artefact-free spectra.[23] The application of time-shared homonuclear decoupling during the acquisition period,[22] using selective pulses of different bandwidth, allowed the extraction of the coupling constant for one linkage and facilitated the measurement in other cases. When the signals for the $^{13}$C nuclei destined for selective excitation are overlapping, the 2D EXSIDE experiment[26] is a good alternative, with the coupling constants easily measured in the $F_1$ dimension, using a scaling factor, without influence of a homonuclear coupling. The values of the long-range heteronuclear coupling constants related to the $\phi$ and $\psi$ dihedral angles of the oligosaccharides were 3.6–4.3 and 4.3–5.3 Hz, respectively. For the two trisaccharides, and also for their constituent disaccharides, the values of $^3J$(C,H) for the $\phi$ dihedral angles were systematically underestimated in all the computer simulations whereas $^3J$(C,H) for the $\psi$ dihedral angles showed better and in many cases good agreement with simulated data. This may be explained by the fact that the same Karplus equation is used for calculations at both the $\phi$ and the $\psi$ dihedral angles even though substituents at these two angles differ, i.e. oxygen *vs.* carbon. The site-specific deuteration in methyl $\beta$-cellobioside made it possible to reveal a larger value of $^3J$(C,H) than reported earlier, indicating that an '*anti*'-conformer in the $\psi$ dihedral angle may be present to a larger degree than previously estimated, a result that can be interpreted as an increased flexibility at the glycosidic linkage of cellobiose, emphasizing the need for accurate experimental data.

## Acknowledgements

This work was supported by a grant from the Swedish Natural Science Research Council. The authors are grateful to Professor Ray Freeman, Dr Frederico del Rio-Portilla (University of Cambridge) and Dr Ēriks Kupče (University of Oxford) for their advice and helpful suggestions and for the $J$-doubling and Pandora's Pulse Box programs.

## REFERENCES

1. J. Dabrowski and L. Poppe, *J. Am. Chem. Soc.* **111**, 1510 (1989).
2. M. Karplus, *J. Chem. Phys.* **30**, 11 (1959).
3. B. Mulloy, T. A. Frenkiel and D. B. Davies, *Carbohydr. Res.* **184**, 39 (1988).
4. I. Tvaroska, M. Hricovíni and E. Petráková, *Carbohydr. Res.* **189**, 359 (1989).
5. P. E. Hansen, *Prog. Nucl. Magn. Reson. Spectrosc.* **14**, 175 (1981).
6. C. Morat and F. R. Taravel, *Tetrahedron Lett.* **29**, 199 (1988).
7. T. E. Walker, R. E. London, T. W. Whaley, R. Barker and N. A. Matwiyoff, *J. Am. Chem. Soc.* **98**, 5807 (1976).
8. G. K. Hamer, F. Balza, N. Cyr and A. S. Perlin, *Can. J. Chem.* **56**, 3109 (1978).
9. A. Bax and R. Freeman, *J. Am. Chem. Soc.* **104**, 1099 (1982).
10. G. Batta and A. Lipták, *J. Chem. Soc., Chem. Commun.* 368 (1985).

 

11. D. Uhrín, A. Mele, J. Boyd, M. R. Wormald and R. A. Dwek, *J. Magn. Reson.* **97**, 411 (1992).
12. G. Zhu and A. Bax, *J. Magn. Reson. A* **104**, 353 (1993).
13. T. J. Norwood, J. Boyd, J. E. Heritage, N. Soffe and I. D. Campbell, *J. Magn. Reson.* **97**, 488 (1990).
14. V. Blechta, F. del Río-Portilla and R. Freeman, *Magn. Reson. Chem.* **32**, 134 (1994).
15. L. Poppe and H.v. Halbeek, *J. Magn. Reson.* **92**, 636 (1991).
16. B. Adams and L. Lerner, *J. Magn. Reson. A* **103**, 97 (1993).
17. D. Uhrín, A. Mele, K. E. Kövér, J. Boyd and R. A. Dwek, *J. Magn. Reson. A* **108**, 160 (1994).
18. T. Fäcke and S. Berger, *Magn. Reson. Chem.* **33**, 144 (1995).
19. H. Green and R. Freeman, *J. Magn. Reson.* **93**, 93 (1991).
20. E. Kupce and R. Freeman, *J. Magn. Reson. A* **105**, 310 (1993).
21. J. Schraml, H. van Halbeek, A. D. Bruyn, R. Contreras, M. Maras and P. Herdewijn, *Magn. Reson. Chem.* **35**, 883 (1997).
22. T. Nishida, G. Widmalm and P. Sándor, *Magn. Reson. Chem.* **33**, 596 (1995).
23. T. Nishida, G. Widmalm and P. Sándor, *Magn. Reson. Chem.* **34**, 377 (1996).
24. G. Zhu, A. Renwick and A. Bax, *J. Magn. Reson. A* **110**, 257 (1994).
25. G. Xu and J. S. Evans, *J. Magn. Reson. A* **123**, 105 (1996).
26. V. V. Krishnamurthy, *J. Magn. Reson. A* **121**, 33 (1996).
27. J. Stonehouse and J. Keeler, *J. Magn. Reson. A* **112**, 43 (1995).
28. L. McIntyre and R. Freeman, *J. Magn. Reson.* **96**, 425 (1992).
29. Q. Xu, R. Gitti and C. A. Bush, *Glycobiology* **6**, 281 (1996).
30. M. Eberstadt, G. Gemmecker, D. F. Mierke and H. Kessler, *Angew. Chem., Int. Ed. Engl.* **34**, 1671 (1995).
31. W. A. Thomas, *Prog. Nucl. Magn. Reson. Spectrosc.* **30**, 183 (1997).
32. I. Tvaroska and F. R. Taravel, *Adv. Carbohydr. Chem. Biochem.* **51**, 15 (1995).
33. M. T. Duenas-Chasco, M. A. Rodriguez-Carvajal, P. T. Mateo, G. Franco-Rodriguez, J. L. Espartero, A. Irastorza-Iribas and A. M. Gil-Serrano, *Carbohydr. Res.* **303**, 453 (1997).
34. H. Kovacs, S. Bagley and J. Kowalewski, *J. Magn. Reson.* **85**, 530 (1989).
35. S. Bagley, H. Kovacs, J. Kowalewski and G. Widmalm, *Magn. Reson. Chem.* **30**, 733 (1992).
36. J. Kowalewski and G. Widmalm, *J. Phys. Chem.* **98**, 28 (1994).
37. L. Mäler, J. Lang, G. Widmalm and J. Kowalewski, *Magn. Reson. Chem.* **33**, 541 (1995).
38. L. Mäler, G. Widmalm and J. Kowalewski, *J. Biomol. NMR* **7**, 1 (1996).
39. L. Mäler, G. Widmalm and J. Kowalewski, *J. Phys. Chem.* **100**, 17 103 (1996).
40. A. Kjellberg, T. Rundlöf, J. Kowalewski and G. Widmalm, *J. Phys. Chem. B* **102**, 1013 (1998).
41. R. W. Pastor, in *The Molecular Dynamics of Liquid Crystals*, edited by G. R. Luckhurst and C. A. Veracini, p. 85. Kluwer, Dordrecht (1994).
42. B. J. Hardy, W. Egan and G. Widmalm, *Int. J. Biol. Macromol.* **17**, 149 (1995).
43. T. Peters, B. Meyer, R. Stuike-Prill, R. Somorjai and J.-R. Brisson, *Carbohydr. Res.* **238**, 49 (1993).
44. P.-E. Jansson, A. Kjellberg, T. Rundlöf and G. Widmalm, *J. Chem. Soc., Perkin Trans. 2* 33 (1996).
45. P.-E. Jansson, L. Kenne and H. Ottosson, *J. Chem. Soc. Perkin Trans. 1* 2011 (1990).
46. C. Hällgren and G. Widmalm, *J. Carbohydr. Chem.* **12**, 309 (1993).
47. E. Kupce and R. Freeman, *J. Magn. Reson. A* **105**, 234 (1993).
48. J. Friedrich, S. Davies and R. Freeman, *J. Magn. Reson.* **75**, 390 (1987).
49. E̅. Kupče, J. Boyd and I. D. Campbell, *J. Magn. Reson. B* **106**, 300 (1995).
50. F. del Río-Portilla, V. Blechta and R. Freeman, *J. Magn. Reson.* **111**, 132 (1994).
51. L. Emsley and G. Bodenhausen, *J. Magn. Reson.* **97**, 135 (1992).
52. H. Thøgersen, R. U. Lemieux, K. Bock and B. Meyer, *Can. J. Chem.* **60**, 44 (1982).
53. M. L. C. E. Kouwijzer and P. D. J. Grootenhuis, *J. Phys. Chem.* **99**, 13 426 (1995).
54. B. R. Brooks, R. E. Bruccoleri, B. D. Olafson, D. J. States, S. Swaminathan and M. Karplus, *J. Comput. Chem.* **4**, 187 (1983).
55. R. Stuike-Prill and B. Meyer, *Eur. J. Biochem.* **194**, 903 (1990).
56. D. Neuhaus, G. Wagner, M. Vasák, H. R. Kägi and K. Wüthrich, *Eur. J. Biochem.* **151**, 257 (1985).
57. B. J. Hardy, S. Bystricky, P. Kovac and G. Widmalm, *Biopolymers* **41**, 83 (1997).
58. Z.-Y. Yan, B. N. N. Rao and C. A. Bush, *J. Am. Chem. Soc.* **109**, 7663 (1987).
59. G. Widmalm, R. A. Byrd and W. Egan, *Carbohydr. Res.* **229**, 195 (1992).
60. T. Weimar, S. L. Harris, J. B. Pitner, K. Bock and M. Pinto, *Biochemistry* **34**, 13 672 (1995).
61. C. Landersjö, R. Stenutz and G. Widmalm, *J. Am. Chem. Soc.* **119**, 8695 (1997).
62. C. Höög and G. Widmalm, *Glycoconj. J.* **15**, 183 (1998).
63. I. Backman, B. Erbing, P.-E. Jansson and L. Kenne, *J. Chem. Soc., Perkin. Trans. 1* 889 (1988).
64. B. J. Hardy and A. Sarko, *J. Comput. Chem.* **14**, 831 (1993).
65. B. J. Hardy and A. Sarko, *J. Comput. Chem.* **14**, 848 (1993).
66. J. Dabrowski, T. Kozár, H. Grosskurt and N. E. Nifant'ev, *J. Am. Chem. Soc.* **117**, 5534 (1995).
67. B. J. Hardy, A. Gutierrez, K. Lesiak, E. Seidl and G. Widmalm, *J. Phys. Chem.* **100**, 9187 (1996).